Polymer Bulletin 57, 889–899 (2006)
DOI 10.1007/s00289-006-0650-z

Polymer Bulletin

Structure and Mechanical Properties of Shape Memory Polyurethane Based on Hyperbranched Polyesters

Qi Cao (✉), Pengsheng Liu (✉)

College of Chemistry, Xiangtan University, Xiangtan 411105, Hunan Province, P. R. China
E-mail: wjcaoqi@163.com; lpsh@xtu.edu.cn; Fax: +86 732 8292477

Received: 12 April 2006 / Revised version: 2 June 2006 / Accepted: 10 July 2006
Published online: 27 July 2006 –

Summary

Hyperbranched shape memory polyurethane (HB-SMPU) were prepared from 4,4'-diphenylmethane diisocyanate, poly (butylenes adipate) glycol, and hyperbranched polyester as chain extender via a two-step process. The morphology of the HB-SMPU films was investigated by the use of wide-angle X-ray diffraction (WAXD), atomic force microscopy (AFM), DSC and dynamic mechanical analysis (DMA). It was found that the PBAG soft segments in HB-SMPU with 15-35 wt.% of hard segments were in a crystalline state, however, the PBAG segments were in an amorphous state in the HB-SMPU with 40 wt.% hard segments. The increase of the hard segment content resulted in the decrease of the melt transition temperature of the HB-SMPU. The HB-SMPU with 25 wt. % of hard segment content possessed highest loss tangent. Heat of crystallization was dependent on the content of hard segment in the HB-SMPU. 96-98% shape recovery could be obtained for the HB-SMPU with 15-35 wt.% of hard segment. The content of hard segments in HB-SMPU was very important in determining their physical properties.

Introduction

Intelligent materials will play a prominent role in the future [1]. In the last few years, this concept has found growing interest as a result of the broad application of shape memory materials in the intelligence or alertness fields [1-3]. Shape memory materials mainly include shape memory ceramics, shape memory metal alloys and shape memory polymers (SMP) [3]. Compared to metallic alloys, shape memory polymers show more structural versatility, lower manufacturing cost, easier pretreatment procedure, larger recoverable deformation, and lower recovery temperature. Therefore SMP have found wide industrial applications in the field of heat-shrinkable materials [4,5]. And they are expected to get more intelligence so as to be used in self-healing or other high-tech application fields [6]. Shape memory polyurethane (SMPU), as a typical thermo-sensitive smart polymer with excellent shape memory behavior, has been extensively studied in the past decade [1-3,7-11].

It is well known that SMPU has a micro-phase separated supra-structure, where the SMPU basically consists of two phases, a frozen phase and a reversible phase. The hard segments of SMPU aggregate together via strong hydrogen bonding to form stable dispersed domains that act as physical cross-linkers (frozen phase). Whereas,

soft segmental matrix (reversible phase) is mainly responsible for the shape memory behavior of SMPU, therefore the shape memory behavior can be tuned through the manipulation of the soft segments, such as the ratio of hard/soft segments and polymerization procedure [2,7-8]. In the most recent decade, dendritic polymer has been intensively studied due to its special properties and potential applications in the field of biomedical engineering, catalysis and commercial coatings [12-25]. As a kind of special dendritic polymer, hyperbranched polyurethane (HB-PU) was first prepared by Spindler and Fréchet [26] using thermally labile blocked isocyanates. Then several dielectric relaxation studies on the linear and branched PU systems have been published in the literature [27-29]. Roussos et al. investigated novel linear/low-branched polyurethane by means of dielectric techniques [30]. Recently broad attentions have been paid to the polyurethane systems with hyperbranched polymers that were incorporated in a PU matrix as blends [31] or introduced in the network as a precursor [32,33]. However, to the best of our knowledge, SMPU with hyperbranched polyester as chain extender has never been reported before.
In this paper, we report the synthesis of novel SMPU using hyperbranched polyester (Boltorn®H30, the third generation, Sweden) as a precursor. And the thermo-sensitive shape memory properties and supra-structures of the obtained HB-SMPU are also investigated in details.

Experimental

Materials

Boltorn®H30 (Third generation, M_w = 3,500 g/mol, hydroxyl number equals 470-500 mg KOH/g, Sweden) was purchased from Perstorp Specialty Chemicals, dried at 60°C under vacuum for overnight prior to use. Poly (butylene adipate) glycol (PBAG, M_n = 2000 g/mol, purchased from Aldrich) was used without further purification. 4,4'-Diphenylmethane diisocyanate (MDI, purchased from Yantai Synthetic Leather General Factory) was heated to 60°C and kept at temperature for 2 h and then filtered through a heated filter.

Synthesis of HB-SMPU

The synthesis route for hyperbranched polyurethane (HB-SMPU) is shown in Scheme 1. While the feed ratios of the obtained PU polymers are summarized in Table 1. The general procedure is as follows: dehydrated PBAG and excess of MDI solution (20 wt. %) in freshly distilled DMF were charged into a 250-ml three-necked round-bottom flask equipped with magnetic stirrer. The reaction mixture was stirred under reduced pressure at 80°C for 3 h. Then Boltorn®H30 solution in dried DMF was added to the reaction mixture. After stirring for another 2 h, the reaction mixture was cast into glass pan and placed under vacuum at 60°C for 1 h. The solvent was removed under vacuum and then further polymerization was carried out in an oven at 80°C for 24 h. The polymers were obtained as films with a thickness of 0.2-1.0 mm.

Preparation of HB-SMPU Solution for AFM

The samples were prepared as follows: PU was dissolved in DMF to give a 0.5 wt. % diluted solution. 2μL solution was deposited on a freshly cleaned silicone wafer via

spin coating, followed by keeping it at 80°C in an oven for 30 min. The specimens were cooled down at room temperature prior to measurement.

Table 1. Synthesis parameters for HB-SMPU with different compositions

Soft Segment (Mn, g mol-1)	Chain extender	[NCO]/[OH][a]	HS content[b] (wt.%)
PBAG2000	H30	1.00	15
PBAG2000	H30	1.00	20
PBAG2000	H30	1.00	25
PBAG2000	H30	1.00	30
PBAG2000	H30	1.00	35
PBAG2000	H30	1.00	40

HS: hard segments; HS content = $[(W_{MDI} + W_{H30}) / (W_{MDI} + W_{H30} + W_{PBAG})] * 100\%$;
(a) feed molar ratio of isocyanate groups to hydroxyl groups;
(b) calculated according the feed weight ratio.

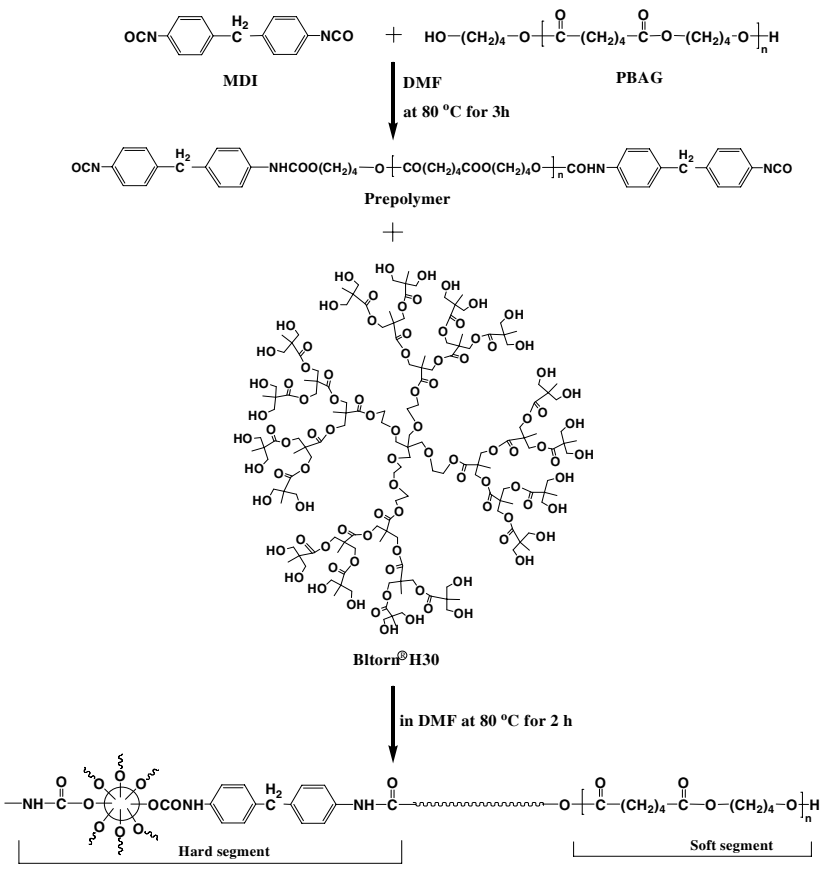

Scheme 1. Synthesis of HB-SMPU

Characterization

Wide-angle X-ray diffraction (WAXD) was employed for studying the phase morphology by using a Philip PW 1710 at 30 kV and 20mA. WAXD studies were carried out with samples of 1mm thickness and with Bragg's angle 2θ from 10 to 50° at the rate of 3°/min.

Tapping-mode atomic force microscopy (AFM) was used to visualize the images of SMPU on a DI Nanoscope IIIa AFM, Micro-fabricated cantilevers or silicon probes (Nanoprobes, Digital Instruments) with 125μm long cantilevers were used at their fundamental resonance frequencies, which typically varied from 270 to 350 kHz depending on the cantilever. Cantilevers had a very small tip radius of 5-10 nm. The AFM was operated at ambient with a double-vibration isolation system. Extender electronics were used to obtain height and phase information simultaneously. The lateral scan frequency was about 1.5 Hz.

Differential scanning calorimetry (DSC) of the obtained HB-SMPU was carried out using a 2920 TA Instrument. Samples (ca. 10mg) were sealed in aluminum pans and measurements were performed in nitrogen atmosphere at a heating rate of 10°C /min in the temperature range of -50-150°C. In the first scanning, the sample was heated to 150°C, kept at this temperature for 5 min, and cooled to -50°C at a cooling rate of 20°C/min. In the second scanning, the sample was heated again to 150°C, and the second scan was recorded.

Thermo-gravimetric analysis (TGA) was carried out in Dupont TGA 2950 at a scanning rate of 20°C/min from 25°C to 500°C.

Shape memory behavior studies Rectangular specimens with 20 mm length, 5 mm width and 0.5 mm thickness were prepared for these measurements. Stretching the film to the elongation of 300 % at 60°C ($T>T_m$ of the soft-segment domains), quickly cooled down to 0°C under stretching conditions. The specimens were then placed on the desk at 25°C for 5 min. The strain recovery was measured in an oil bath with a hot stage at a heating rate of 2.5°C /min. The length at different conditions was recorded, then the shape recovery (R_T), maximum shape recovery (R_{max}), shape fixity (F) are defined as follows:

$$R_T = (L_S-L_T) / (L_S-L_0)*100\% \quad (1)$$

$$R_{max} = (L_S-L_R) / (L_S-L_0)*100\% \quad (2)$$

$$F= (L_F-L_0) / (L_{max}-L_0)*100\% \quad (3)$$

Where, L_0 is the original length, L_{max} is the maximum stretched length, L_F is the fixed length at 0°C, L_S is the stable length at ambient temperature, L_T is the length at a certain temperature (T) during the heating process, L_R is the recovery length.

Results and Discussions

X-ray diffraction studies

As reported in the literature [34], the pure PBAG showed three peaks at 2θ = 21.5˚, 22˚and 24˚ in the X-ray diffraction pattern. Whereas, the crystallization of PBAG segments was disturbed pronouncedly in the PU, due to the hindrance of hard segments [35]. As shown in Fig. 1, a very diffused diffraction peak near 2θ = 21.5˚ appeared for all polyurethane of different hard segment content, and its intensity

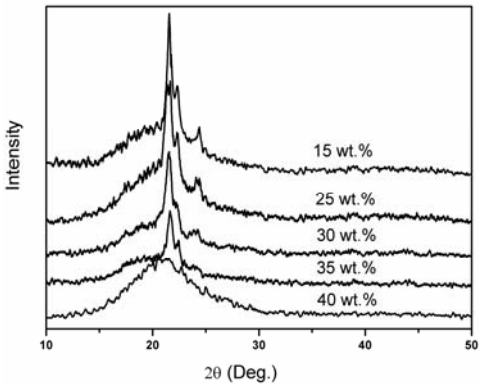

Fig. 1. WAXD profiles of the HB-PU with various hard segment contents

gradually decreased as increasing the hard segment content. They appeared to be associated with PBAG crystallization. These indicated that they have the same crystal structure and unit cell type, and that the crystallization of the HB-SMPU was disturbed with the increase of hard segment content. So it was reasonable that the diffraction profiles of the HB-SMPU with 40 wt% hard segments finally evolved to a broad amorphous hale. These results were in good agreement with the DSC results as to be discussed below.

Atomic force microscopy studies

The morphology of HB-SMPU was visualized using a tapping-mode AFM (see Fig.2). For a moderate force image, the high phase corresponded to high modulus; therefore, the lighter phases were richer in polyurethane, while the darker phases corresponded to the polyol phase. We used a conventional interpretation of modulus-sensitive phase images at light tapping where the lighter color portions were assigned to the organized domain, i.e., the MDI-H30 hard block and the crystallites of soft segments. Furthermore, one can see that the hard segment domains fill space relatively

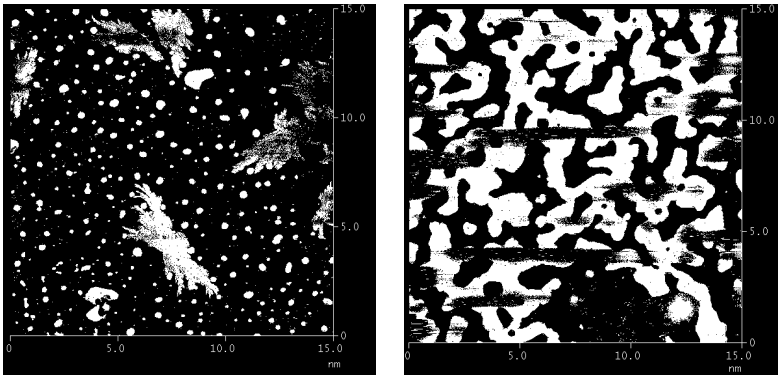

(a) (b)

Fig. 2. Tapping-mode AFM height images of HB-PU with various hard segment content: (a) 25wt% (b) 40wt%

uniformly with no gross regions free of hard segment domains. The AFM image reveals the connected hard-segment domains. This was in general agreement with AFM images reported in the literatures [36]. Importantly, the AFM image of HB-SMPU with 25 wt% hard segments (see Fig. 4a) showed the existence of crystallites, whereas no crystallites was observed from the image of HB-SMPU with 40 wt% hard segments (Fig. 4b). This was in general agreement with the DSC and WAXD results. The crystallites of soft segment made phase separation pronounced. But the crystallization of the reversible phase was disturbed with the increase of hard segment content in the HB-SMPU.

Thermal properties

The DSC traces of HB-SMPU were shown in Fig. 3. The crystalline soft segment melting temperatures (T_m) are summarized in Table 2. No thermo-transition was observed at 100-200°C (data not shown). It was evident that the hard segment contents had influence on melting temperature of the soft segments, the melting behavior of crystallites was less pronounced with the increasing hard segments of HB-SMPU. The samples with higher percentage of hard segments showed rather smaller heat of transition at the melting temperature (T_m), suggesting that more ordered polymer package was obtained at low percentage of hard segment. The melting transition of the crystalline hard segments was not observed due to more flexible backbone structure of hard segments in hyperbranched polyester by comparison with the conventional PU with low molecular weight dibasic alcohol chain extenders. At high temperature, e.g., above 200°C, thermoplastic polyurethane underwent degradation first via decomposition of urethane bonds, followed by breakage of the soft segment phase [37,38]. Such degradation process could be easily monitored by thermo gravimetric analyses (TGA) [39].

In nitrogen, degradation is a two-step process, clearly illustrated in Fig. 4. Results show that the distinct degradation temperature of this HB-SMPU with 25 wt % hard segments at maximum weight loss rate is 424.2°C. Thereat, the thermal stability of this HB-SMPU is very good.

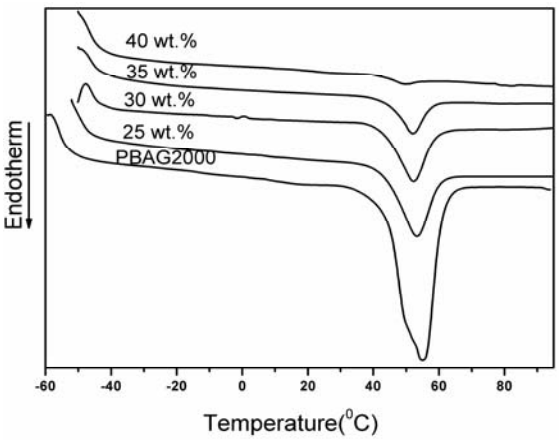

Fig. 3. DSC traces for HB-PU with various hard segments content

Table 2. Thermal properties of HB-SMPU

Material	Tm	Δ Hm (J/g)
PBAG	60.907	101.9
25 wt.%	52.357	38.14
30 wt.%	51.137	36.90
35 wt.%	50.947	25.71
40 wt.%	49.265	5.88

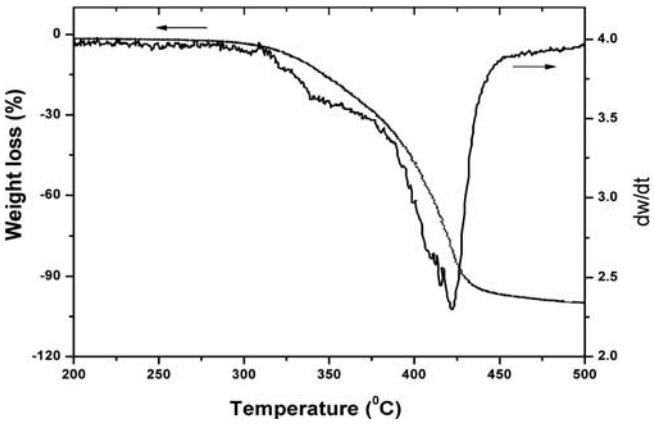

Fig. 4. TGA thermo-grams derivative curves of HB-SMPU with 25 wt.% of hard segment

Dynamic mechanical analysis

The effect of different hard segments on storage modulus (E') and tanδ of HB-SMPU was shown in Fig. 5. The hard segment content of HB-SMPU had a significant influence on the storage modulus. Except for the sample with 40 wt.% hard segments, the increase of the hard segment content led to the decline of storage modulus and melting temperature of PBAG segments in the HB-SMPU. In the region of melting temperature of PBAG segments, storage modulus of HB-SMPU decreased sharply with the increase of temperature (Fig. 5a). Such a decrease of storage modulus in PU was not uncommon [2]. If the soft segment PBAG could crystallize, it would show different modulus value with each different degree of crystallization at low temperature [40]. Hence, the soft segments of the studied samples were in the crystalline state, which was further confirmed by the studies of DSC and WAXD. The E' and tanδ curves of 40 wt.% HB-SMPU all were straight line in the range of 0-80°C (Fig.5), suggesting predominantly amorphous soft segment phase in the hyperbranched polyurethane, which was matched with the DSC and WAXD results. The tanδ curves of samples were shown in Fig. 5b. The tanδ reflected the movement of molecular chain. Since all molecular chains segment were froze at glass state, the tanδ at glass state ($tan\delta_g$) was low and only changed slightly. However the micro-Brown movement of soft segment was quickened after the crystal melting, so that the tanδ at rubber state ($tan\delta_r$) improved greatly and the difference emerged accordingly. The soft segmental mobility (α transition) was observed at ca. 50°C. Loss tangent for the HB-SMPU decreased with the increasing hard segment, so that the highest loss tangent value of 0.65 was obtained from the HB-SMPU with 25 wt. % of hard

segment. Damping effect at T_m was known to be dependent heavily on the hard segment content and crystallization of soft segment [41-43]. The best damping effect could be expected for the HB-SMPU with 25 wt. % of hard segment content. As shown in Fig. 4b, the HB-SMPU displayed one distinct transition that corresponded to the melt transition of the soft segment phase. With the increasing of the wt.% of hard segment, the melt transition of the PBAG phase moved towards the low temperature and the peak width became broad, which indicated that there was a certain interaction existed between the soft segment and hard segment molecular chain.

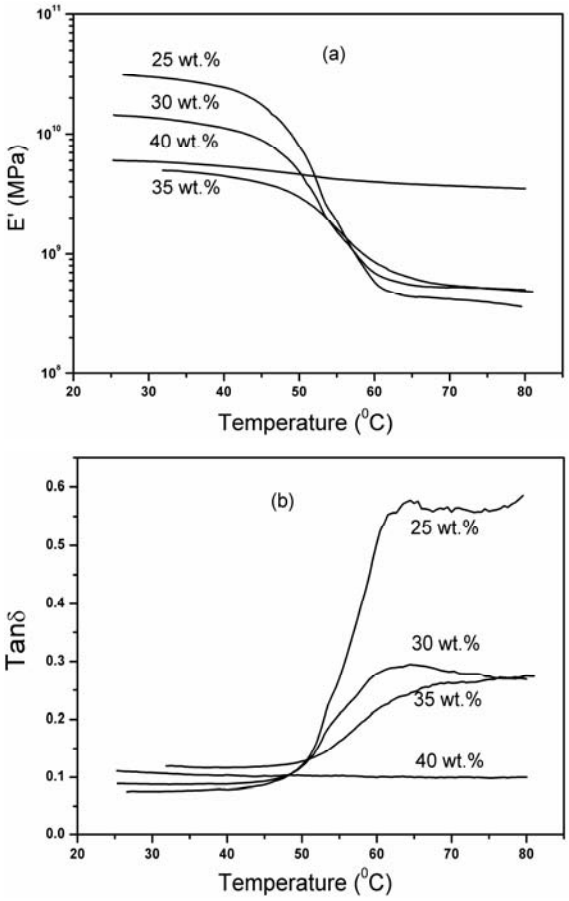

Fig. 5. Storage modulus ($E^{'}$) and Tanδ of HB-PU with various wt.% of hard segment as a function of temperature

Shape memory behavior studies

Long soft segments and suitable hard segment contents were necessary for SMPU with high final recovery memory behavior. The recovery temperature (T_r) was related to the reversible phase transition temperature that was contributed by the melting process of soft segment matrix in SMPU. As shown in Fig. 6, it was observed that the T_r moved towards low temperature with the increase of the wt.% of hard segment.

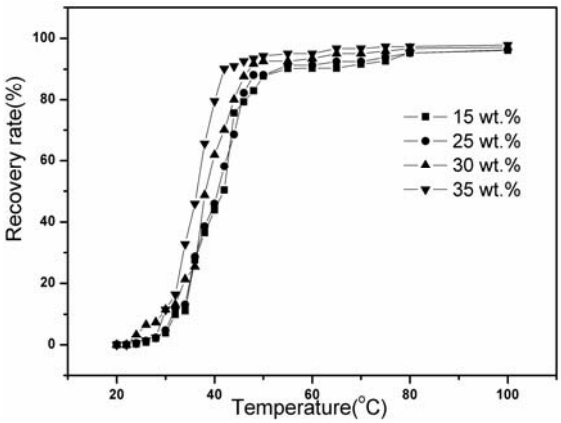

Fig. 6. Strain recovery curves of the HB-SMPU with various hard segment contents

This confirmed that there was a certain interaction existing between the soft segment and hard segment molecular chain. And the interaction became strong with increasing wt.% of hard segment, which made the T_r moving towards the low temperature. As shown in Fig. 6, the maximum recovery rate (R_{max}) of HB-SMPU depended on the hard segment contents. It was worthy noted that all of the HB-SMPU had excellent recovery rate (R_{max} > 96%). These indicated that there was strong interaction or physical cross-link existed in the HB-SMPU, which resulted in the good shape memory effect. Stabilization of the PU through dipole-dipole interaction, hydrogen bonding, and induced dipole-dipole interaction of the hard segments were believed to be responsible for the high shape recovery rate at above T_m of PBAG segments. Thus, it could be concluded that 96-98% of maximum shape recovery was able to be obtained for the HB-SMPU with 15-35 wt % of hard segment content where PU copolymers had strong interaction among hard segments enough to restore the polymer back to the original shape. In the long run, we would like to use the shape memory PU for the development of smart fabric that would be able to control moisture and/or smart fiber-reinforced composite with damping capability.

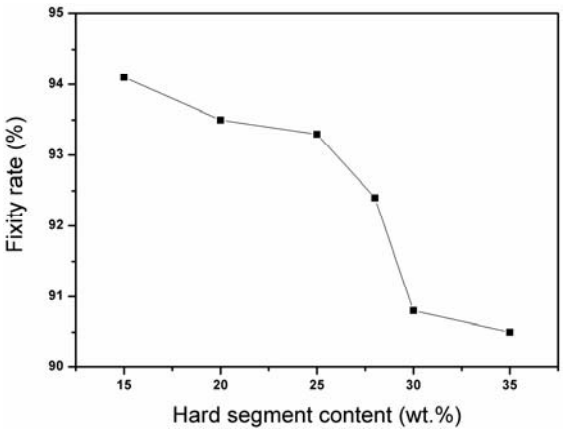

Fig. 7. Fixity rate of the HB-SMPU with various hard segment contents

The relationship between fixity rate of the HB-SMPU and hard segment contents is shown in Fig. 7, the fixity rate of HB-SMPU decreases with increasing hard segment content, which implies that the increase of hard segment content enhances the rigidity of HB-SMPU. Strain recovery process are really the macroscopically reflection of microstructure. From the analysis above, it is known that the micro-Brown movement of soft segment has a great influence on the strain recovery temperature, while the storage modulus change at T_m usually influences the fixity rate.

Conclusions

Crystallinity of soft segments in the HB-SMPU decreased with increasing hard segment content. The highest loss tangent was observed for HB-SMPU with 25 wt% hard segments, which suggested the importance of the combination of hard segment and soft segment. The AFM image for HB-SMPU with 25 wt% hard segments showed the existence of crystallites, but no crystallite was observed from the image for HB-SMPU with 40wt% hard segment content, which was also supported by the results of DSC and WAXD measurements. This suggested that the crystallization of the reversible phase was disturbed with the increase of hard segment content in the HB-SMPU. Heat of crystallization measured by differential scanning calorimetry was also dependent on the hard segment content. The control of hard segment content in HB-SMPU was very important in determining their physical properties. 96-98% of maximum shape recovery was able to be obtained for the HB-SMPU with 15-35 wt.% of hard segment content. Further work including modification of PU is underway in our laboratory.

Acknowledgements. The Science Research Foundation from Education Department of Hunan Province, P. R. China, subsidized this work.

References

1. Wang MT, Zhang, LD (1999) J Polym Sci B: Polym Phy 37: 101.
2. Lee BS, Chun BC, Chung YC, Sul KI, Cho JW (2001) Macromolecules 34: 6431.
3. Du ZG, Zhu GM, Qin RF, Zhou HF, Zhang LB (2004) China Plastics 18: 6.
4. Kleinhans G, Starkl W, Nuffer K (1984) Kunststoffe 74: 445.
5. Kleinhans G, Heidenhain F (1986) Kunststoffe 76: 1069.
6. Lendlein A, Kelch S (2002) Angew Chem Int Ed 41: 2034.
7. Kim BK, Lee SY, Xu M (1996) Polymer 37: 5781.
8. Li FK, Zhang X, Hou J, Xu M, Luo XL, Ma DZ, Kim BK (1997) J Appl Polym Sci 64: 1511.
9. Kim BK, Lee SY, Lee JS, Baek SH, Choi YJ, Lee JO, Xu M (1998) Polymer 39: 2803.
10. Kim BK, Shin YJ, Cho SM, Jeong HM (2000) J Polym Sci B: Polym Phys 38: 2652.
11. Jeong HM, Ahn BK, Cho SM, Kim BK (2000) J. Polym. Sci. B: Polym Phys 38: 3009.
12. Breton MP (1998) US Patent 5266106.
13. Winnik FM (1998) US Patent 5098475.
14. Tomalia DA, Naylor AM, Goddhard WA (1990) Angew Chem Int Ed Engl 29: 138.
15. Kim YH, Webster OW (1992) Macromolecules 25: 5561.
16. Inoue K (2000) Prog Polym Sci 25: 453.
17. Fréchet JMJ, Tomalia DA (2001) Dendrimers and other dendritic polymers. West Sussex: Wiley.
18. Desimone JM (1995) Science 269: 1060.
19. Yates CR, Hayes W (2004) Eur Polym J 40: 1257.

20. Malmstrom E, Johansson M, Hult A (1995) Macromolecules 28: 1698.
21. Percec V, Kawasumi M (1992) Macromolecules 25: 3843.
22. Uhrich KE, Boegeman S, Fréchet JMJ, Turner SR (1991) Polym Bull 25: 551.
23. Spindler R, Fréchet J (1993) M. J. Macromolecules 26: 4809.
24. Miravet JF, Fréchet JMJ (1998) Macromolecules 31: 3461.
25. Van Benthem RATM, Muscat D, Stanssens DAW (1999) Polym Mater Sci Eng 80: 72.
26. Spindler R, Fréchet JMJ (1993) Macromolecules 26: 4809.
27. Frubing P, Kruger H, Goering H, Gerhard-Multhaupt R (2002) Polymer 43: 2787.
28. Savelyev YV, Arhranovich ER, Grekov AP, Privalko EG, Korskanov VV, Shtompel VI, Privalko VP, Pissis P, Kanapitsas A (1998) Polymer 39: 3425.
29. Pissis P, Kanapitsas A, Savelyev YV, Arhranovich ER, Privalko EG, Privalko VP (1998) Polymer 39: 3431.
30. Roussos M, Konstantopoulou A, Kalogeras IM, Kanapitsas A, Pissis P, Savelyev YV, Vassilikou-Dova A (2004) E-Polym, art no. 042.
31. Jahromi S, Litvinov V, Coussens B (2001) Macromolecules 34: 1013.
32. Nasar AS, Jikei M, Kakimoto M (2003) Eur Polym J 39: 1201.
33. Okrasa L, Zigon M, Zagar E, Czech P, Boiteux G (2005) Journal of Non-Crystalline Solids 351: 2753.
34. Lin LR, Chen LW (1999) J Appl Polym Sci 73: 1305.
35. Blackwell J, Gardner K H (1979) Polymer 20: 13.
36. Wu L, Ryan AJ (2002) Macromolecules 35: 5034.
37. Yang WP, Macosko C W, Wellinghoff ST, Yang WP, Macosko CW, Wellinghoff ST (1986) Polymer 27: 1235.
38. Petrovic ZS, Zavargo Z, Flynn JH, Macknight WJ (1994) J Appl Polym Sci 51: 1087.
39. Chang CT, Shen WS, Chiu YS (1995) Polym Degrad Stab 49: 353.
40. Li F, Zhang X, Hou J, Xu M, Lou X, Ma D, Kim BK (1997) J Appl Polym Sci 64: 1511.
41. Takahashil T, Hayashi N, Hayashi SJ (1996) Appl Polym Sci 60: 1061.
42. Pissis P, Apekis L, Christtodoulides C, Niaounakis M, Kyritsis A, Nedbal JJ (1996) Polym Sci Part A: Polym Phys 34: 1529.
43. Seo BS, Lee HS, Jin MJJ (1997) Polym Sci 34: 148.